E-ISSN:2250-0758
P-ISSN:2394-6962
Research Article
Induction Motor

International Journal of Engineering and Management Research

2025 Volume 15 Number 6 December

Publisher
Vandana Publications
www.vandanapublications.com

Comparative Analysis of Induction Machine Performance Under Balanced/Unbalanced Conditions Using MATLAB Simulink

Salihu J[1*], Chukwuma O[2], Akpama E[3]

DOI:10.5281/zenodo.17899251

[1*] John Salihu, Department of Electrical and Electronic Engineering, Cross Rivers State University, Calabar, Nigeria.

[2] Osita Chukwuma, Consultant, DGS Technologies, United Kingdom.

[3] Eko Akpama, Professor, Department of Electrical and Electronic Engineering, Cross Rivers State University, Calabar, Nigeria.

This study investigates the dynamic performance of a three-phase induction motor across stationary, rotor, and synchronous reference frames. It evaluates torque-speed characteristics under balanced and unbalanced supply voltage conditions to identify the most appropriate reference frame for simulation in scenarios involving voltage imbalances. The analysis employs park's transformation to simplify the modelling process, with simulations conducted in MATLAB/Simulink. Flux linkage equations derived from the motor parametric voltage equations are integrated into an embedded MATLAB functions to model the motor's dynamic behaviour. Results reveal that the synchronous reference frame is optimal for balanced conditions, the rotor frame for unbalanced stator voltages, and the stationary frame for unbalanced rotor voltages. Torque-speed profiles remain consistent across frames under balanced voltages, highlighting the robustness of the d-q transformation modelling approach.

Keywords: Induction Motor, Reference Frames, Balanced and Unbalanced Voltages, Dynamic Simulation, d-q Transformation

Corresponding Author

John Salihu, Department of Electrical and Electronic Engineering, Cross Rivers State University, Calabar, Nigeria.
Email: johnsalihu@unicross.edu.ng

How to Cite this Article

Salihu J, Chukwuma O, Akpama E, Comparative Analysis of Induction Machine Performance Under Balanced/Unbalanced Conditions Using MATLAB Simulink. Int J Engg Mgmt Res. 2025;15(6):10-16. Available From https://ijemr.vandanapublications.com/index.php/j/article/view/1819

To Browse

Manuscript Received	Review Round 1	Review Round 2	Review Round 3	Accepted
2025-11-02	2025-11-19			2025-12-03

Conflict of Interest	Funding	Ethical Approval	Plagiarism X-checker	Note
None	Nil	Yes	6.54	

1. Introduction

Extensive research has been carried out on the behaviour of induction motors under balanced supply conditions; however, in real-world conditions, voltage imbalances often occur due to line faults or irregularities in the supply. To make analysis easier, d-q transformation is used because it simplifies three-phase systems [1], [2], [3]. Dynamic modelling can be performed in stationary, rotor, or synchronous reference frames, depending on voltage variations and system parameters [4], [5]. Different software are often employed tools to facilitate these simulations [6], [7], with MATLAB/Simulink being particularly effective for analysing electrical machines and drives systems [8], [9]. This paper describes a dynamic d-q model of a three-phase induction motor in state space form and its simulation in MATLAB/Simulink program, [2], [9] to analyze the motor behaviour through mathematical models in different reference frames, evaluating torque and speed responses under both balanced and unbalanced voltages.

2. Mathematical Modelling of the Induction Motor

The induction machine's d-q equivalent circuit is shown in Fig. 1. The model based on this equivalent circuit is Krause's model, detailed in [1], [8]. The induction machine is modelled using Park's transformation to convert a-b-c-phase variables into the d-q reference frame. According to Krause's model, the modelling equations in flux linkage form are as shown below.

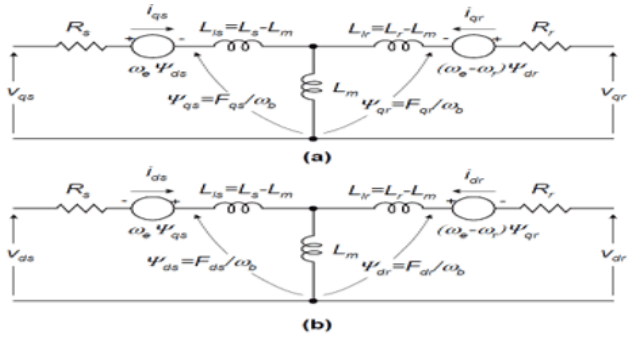

Figure 1: d-q equivalent circuit of an induction machine

$$\frac{dF_{qs}}{dt} = \omega_b \left[v_{qs} - \frac{\omega_e}{\omega_b} F_{ds} + \frac{R_s}{x_{ls}}\left(F_{mq} + F_{qs}\right)\right] \quad (1)$$

$$\frac{dF_{ds}}{dt} = \omega_b \left[v_{ds} + \frac{\omega_e}{\omega_b} F_{qs} + \frac{R_s}{x_{ls}}\left(F_{md} + F_{ds}\right)\right] \quad (2)$$

$$\frac{dF_{qr}}{dt} = \omega_b \left[v_{qr} - \frac{(\omega_e - \omega_r)}{\omega_b} F_{dr} + \frac{R_r}{x_{lr}}\left(F_{mq} - F_{qr}\right)\right] \quad (3)$$

$$\frac{dF_{dr}}{dt} = \omega_b \left[v_{dr} + \frac{(\omega_e - \omega_r)}{\omega_b} F_{qr} + \frac{R_r}{x_{lr}}\left(F_{md} - F_{dr}\right)\right] \quad (4)$$

$$F_{mq} = x^*_{ml}\left[\frac{F_{qs}}{x_{ls}} + \frac{F_{qr}}{x_{lr}}\right] \quad (5)$$

$$F_{md} = x^*_{ml}\left[\frac{F_{ds}}{x_{ls}} + \frac{F_{dr}}{x_{lr}}\right] \quad (6)$$

Where $x^*_{ml} = \frac{1}{\left(\frac{1}{x_m} + \frac{1}{x_{ls}} + \frac{1}{x_{lr}}\right)}$,

$$i_{qs} = \frac{1}{x_{ls}}\left(F_{qs} - F_{mq}\right) \quad (7)$$

$$i_{ds} = \frac{1}{x_{ls}}\left(F_{ds} - F_{md}\right) \quad (8)$$

$$i_{qr} = \frac{1}{x_{lr}}\left(F_{qr} - F_{mq}\right) \quad (9)$$

$$i_{dr} = \frac{1}{x_{lr}}\left(F_{dr} - F_{md}\right) \quad (10)$$

When a squirrel cage induction machine is considered as in this study, v_{qr} and v_{dr} in equations (3) and (4) are set to zero. Consequently, equations (5) and (6) are incorporated into (1 – 4), and like terms are grouped to arrange the equations in state space form[8], [10], [11]. This ensures that each state derivative depends solely on other state variables and model inputs. The equations (1 – 4) for a squirrel cage induction motor in state space then become.

$$\frac{dF_{qs}}{dt} = \omega_b \left[v_{qs} - \frac{\omega_e}{\omega_b} F_{ds} + \frac{R_s}{x_{ls}}\left(\frac{x^*_{ml}}{x_{lr}} F_{qr} + \left(\frac{x^*_{ml}}{x_{ls}} - 1\right)F_{qs}\right)\right] \quad (11)$$

$$\frac{dF_{ds}}{dt} = \omega_b \left[v_{ds} + \frac{\omega_e}{\omega_b} F_{qs} + \frac{R_s}{x_{ls}}\left(\frac{x^*_{ml}}{x_{lr}} F_{dr} + \left(\frac{x^*_{ml}}{x_{ls}} - 1\right)F_{ds}\right)\right] \quad (12)$$

$$\frac{dF_{qr}}{dt} = \omega_b \left[-\frac{(\omega_e - \omega_r)}{\omega_b} F_{dr} + \frac{R_r}{x_{lr}}\left(\frac{x^*_{ml}}{x_{ls}} F_{qs} + \left(\frac{x^*_{ml}}{x_{lr}} - 1\right)F_{qr}\right)\right] \quad (13)$$

$$\frac{dF_{dr}}{dt} = \omega_b \left[\frac{(\omega_e - \omega_r)}{\omega_b} F_{qr} + \frac{R_r}{x_{lr}}\left(\frac{x^*_{ml}}{x_{ls}} F_{ds} + \left(\frac{x^*_{ml}}{x_{lr}} - 1\right)F_{dr}\right)\right] \quad (14)$$

3. D-Q Transformation of Three–Phase Induction Motor

In a balanced three-phase circuit, the application of the d-q transformation converts the three AC quantities into two DC quantities [4], [12], [13]. The steps involved in achieving the d-q transformation are Clarke's and Park's transformations. The three-phase voltages, which vary over time along the a, b, and c axes, are mathematically transformed into two voltages that

vary over time along the α and β axes, according to Clarke, using the transformation matrix in equation (15) [4], [14]. The inverse transformation, which enables the three-phase quantities to be obtained from the two-phase quantities, can be performed using the transformation matrix in equation (16).

$$\begin{bmatrix} V_\alpha \\ V_\beta \end{bmatrix} = \frac{2}{3}\begin{bmatrix} 1 & -\frac{1}{2} & -\frac{1}{2} \\ 0 & \frac{\sqrt{3}}{2} & -\frac{\sqrt{3}}{2} \end{bmatrix}\begin{bmatrix} V_a \\ V_b \\ V_c \end{bmatrix} \quad (15)$$

$$\begin{bmatrix} V_a \\ V_b \\ V_c \end{bmatrix} = \frac{2}{3}\begin{bmatrix} 1 & 0 \\ -\frac{1}{2} & \frac{\sqrt{3}}{2} \\ -\frac{1}{2} & \frac{\sqrt{3}}{2} \end{bmatrix}\begin{bmatrix} V_\alpha \\ V_\beta \end{bmatrix} \quad (16)$$

Park's transformation converts quantities from the two-axis orthogonal stationary reference frame into the rotating frame using the transformation matrix in equation (17). Additionally, transforming the two-phase rotating quantities to a two-phase stationary frame can be achieved with the transformation matrix in equation (18).

$$\begin{bmatrix} V_d \\ V_q \end{bmatrix} = \begin{bmatrix} cos\theta & sin\theta \\ -sin\theta & cos\theta \end{bmatrix}\begin{bmatrix} V_\alpha \\ V_\beta \end{bmatrix} \quad (17)$$

$$\begin{bmatrix} V_\alpha \\ V_\beta \end{bmatrix} = \begin{bmatrix} cos\theta & -sin\theta \\ sin\theta & cos\theta \end{bmatrix}\begin{bmatrix} V_d \\ V_q \end{bmatrix} \quad (18)$$

Balanced voltage equation in the abc reference frame is as follows:

$$V_a = V_m \cos(\omega t) \quad (19)$$

$$V_b = V_m \cos(\omega t + 2\pi f) \quad (20)$$

$$V_c = V_m \cos(\omega t - 2\pi f) \quad (21)$$

While an unbalanced voltage condition in the abc reference frame is as follows:

$$V_a = V_m \cos(\omega t) \quad (22)$$

$$V_b = \frac{3}{2} V_m \cos(\omega t + 2\pi f) \quad (23)$$

$$V_c = V_m \cos(\omega t - 2\pi f) \quad (24)$$

4. Flux Linkage Equations in Various Reference Frames

The d-q axis speed of rotation, ω, is substituted into the voltage equations, and certain simplifications occur when the transformation angle θ is adjusted per frame to be one of the following three angles:

4.1 Stationary Reference Frame

In the stationary reference frame, the d-q axis remains non-rotating, with the speed matching that of the stator, therefore $\omega_e = 0$, and $\theta = 0$. By substituting $\omega_e = 0$ into equation (11 - 14), and $\theta = 0$ into equation (17), we derive the following equations.

$$\frac{dF_{qs}}{dt} = \omega_b\left[v_{qs} - \frac{R_s}{x_{ls}}\left(\frac{x''_{ml}}{x_{lr}}F_{qr} + \left(\frac{x''_{ml}}{x_{ls}} - 1\right)F_{qs}\right)\right] \quad (25)$$

$$\frac{dF_{ds}}{dt} = \omega_b\left[v_{ds} + \frac{R_s}{x_{ls}}\left(\frac{x''_{ml}}{x_{lr}}F_{dr} + \left(\frac{x''_{ml}}{x_{ls}} - 1\right)F_{ds}\right)\right] \quad (26)$$

$$\frac{dF_{qr}}{dt} = \omega_b\left[\frac{\omega_r}{\omega_b}F_{dr} + \frac{R_r}{x_{lr}}\left(\frac{x''_{ml}}{x_{ls}}F_{qs} + \left(\frac{x''_{ml}}{x_{lr}} - 1\right)F_{qr}\right)\right] \quad (27)$$

$$\frac{dF_{dr}}{dt} = \omega_b\left[\frac{-\omega_r}{\omega_b}F_{qr} + \frac{R_r}{x_{lr}}\left(\frac{x''_{ml}}{x_{ls}}F_{ds} + \left(\frac{x''_{ml}}{x_{lr}} - 1\right)F_{dr}\right)\right] \quad (28)$$

4.2 Synchronous Reference Frame

The synchronous reference frame occurs when the d-q axis rotates at synchronous speed, with $\omega_e = \omega_s$ and $\theta = \theta_s$. At this point, $\theta = \omega_{st}$. Therefore, substituting ω_s into equations (11–14) results in equations (29–32).

$$\frac{dF_{qs}}{dt} = \omega_b\left[v_{qs} - \frac{\omega_s}{\omega_b}F_{ds} + \frac{R_s}{x_{ls}}\left(\frac{x''_{ml}}{x_{lr}}F_{qr} + \left(\frac{x''_{ml}}{x_{ls}} - 1\right)F_{qs}\right)\right] \quad (29)$$

$$\frac{dF_{ds}}{dt} = \omega_b\left[v_{ds} + \frac{\omega_s}{\omega_b}F_{qs} + \frac{R_s}{x_{ls}}\left(\frac{x''_{ml}}{x_{lr}}F_{dr} + \left(\frac{x''_{ml}}{x_{ls}} - 1\right)F_{ds}\right)\right] \quad (30)$$

$$\frac{dF_{qr}}{dt} = \omega_b\left[-\frac{(\omega_s - \omega_r)}{\omega_b}F_{dr} + \frac{R_r}{x_{lr}}\left(\frac{x''_{ml}}{x_{ls}}F_{qs} + \left(\frac{x''_{ml}}{x_{lr}} - 1\right)F_{qr}\right)\right] \quad (31)$$

$$\frac{dF_{dr}}{dt} = \omega_b\left[\frac{(\omega_s - \omega_r)}{\omega_b}F_{qr} + \frac{R_r}{x_{lr}}\left(\frac{x''_{ml}}{x_{ls}}F_{ds} + \left(\frac{x''_{ml}}{x_{lr}} - 1\right)F_{dr}\right)\right] \quad (32)$$

4.3 Rotor Reference Frame

The rotor reference frame occurs when the d-q axis rotates at the rotor speed, i.e., $\omega_e = \omega_r$, and additionally, the d-axis aligns with the rotor phase A axis. Therefore, substituting $\omega_e = \omega_r$ in equations (11 – 14) results in equations (33 – 36).

$$\frac{dF_{qs}}{dt} = \omega_b\left[v_{qs} - \frac{\omega_r}{\omega_b}F_{ds} + \frac{R_s}{x_{ls}}\left(\frac{x''_{ml}}{x_{lr}}F_{qr} + \left(\frac{x''_{ml}}{x_{ls}} - 1\right)F_{qs}\right)\right] \quad (33)$$

$$\frac{dF_{ds}}{dt} = \omega_b\left[v_{ds} + \frac{\omega_r}{\omega_b}F_{qs} + \frac{R_s}{x_{ls}}\left(\frac{x''_{ml}}{x_{lr}}F_{dr} + \left(\frac{x''_{ml}}{x_{ls}} - 1\right)F_{ds}\right)\right] \quad (34)$$

$$\frac{dF_{qr}}{dt} = \omega_b\left[\frac{R_r}{x_{lr}}\left(\frac{x''_{ml}}{x_{ls}}F_{qs} + \left(\frac{x''_{ml}}{x_{lr}} - 1\right)F_{qr}\right)\right] \quad (35)$$

$$\frac{dF_{dr}}{dt} = \omega_b\left[\frac{R_r}{x_{lr}}\left(\frac{x''_{ml}}{x_{ls}}F_{ds} + \left(\frac{x''_{ml}}{x_{lr}} - 1\right)F_{dr}\right)\right] \quad (36)$$

So far, the flux linkage equations for three reference frames have been introduced. The electrical torque is described by equation (37), which remains independent of the reference frame. The mechanical motion is outlined by equation (38).

$$T_e = \frac{3}{2}\left(\frac{p}{2}\right)\frac{1}{\omega_b}\left(F_{ds}i_{qs} - F_{qs}i_{ds}\right) \quad (37)$$

$$\frac{d\omega_r}{dt} = \left(\frac{p}{2J}\right)(T_e - T_L) \quad (38)$$

5. Presentation of Results

The induction motor used in this simulation is a 7.5 kW, 460V, 50Hz asynchronous motor with the parameters listed in Table 1 below. To assess the three-phase induction motor across various reference frames under both balanced and unbalanced supply conditions, [15], [16], [17], [18], namely, abc currents (i_{as}, i_{bs}, i_{cs}, i_{ar}, i_{br}, i_{cr},) and the d-q axis currents (i_{ds}, i_{qs}, i_{dr}, i_{qr}), as well as the speed–torque characteristics, the equations of IV were employed. The induction motor was simulated using the Simulink induction motor model shown in Figure 2, from which the results were derived.

Table 1: Induction motor parameters

Parameter	Value
Rated power, P	7.5 kW
Line Voltage, VL	460 v
Rated speed, N	1500 rpm
Rr	0.05837 Ω
Rs	0.09961 Ω
Lm	0.030390 H
Lls	0.000867 H
Llr	0.000867 H
J	0.400000 kgm2
Phase voltage, V	VL/√3 v
P	4
TL	49.73 Nm
f	50Hz

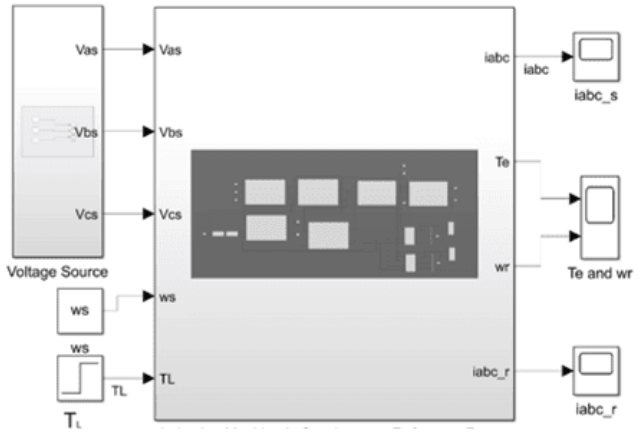

Figure 2: Induction Motor in Synchronous Reference Frame

5.1 Simulation Results and Analysis

The Simulink model of the induction motor, as shown in Fig. 2, was simulated in the MATLAB/Simulink environment.

The results are presented in graphical form through various diagrams. These results include the "abc"-phase stator and rotor currents (ias, ibs, ics, iar, ibr, icr), d-q axis stator and rotor currents (ids, iqs, idr, iqr), and torque-speed profiles under balanced and unbalanced voltage conditions across different reference frames. Table 2 below shows the time for the various quantities (i.e., current, torque and speed) to rise to their maximum value and to attain stability.

Table 2: Time for current, torque and speed to rise to their maximum value and to attain stability

Quantities	Maximum value	Rise time (s)	Steady state value	Time to reach stability (s)
Current (A)	679	0.009	30	0.49
Torque (Nm)	472	0.034	0	0.49
Speed (rad/s)	328	0.354	312	0.49

5.2 Frames of Reference

Figures illustrate the start-up characteristics at no load across each of the three reference frames. The electrical torque (Fig. 3) shows initial 50Hz oscillations, until full speed was attained at 0.49 seconds. The load added at 0.65 seconds, caused the torque and speed to have fluctuated until about 0.75 seconds to attain stability. Although the behaviour of the physical variables in each reference frame is identical, the d-q axis variables in each respective frame differ.

It is worth noting that the torque and speed equations from equations (37) and (38) do not depend on the speed in all three frames of reference. Therefore, the graphs of speed, torque, and speed versus torque in the rotor, stationary, and synchronous reference frames remain unchanged, as shown in fig. 3, 4, and 5 below.

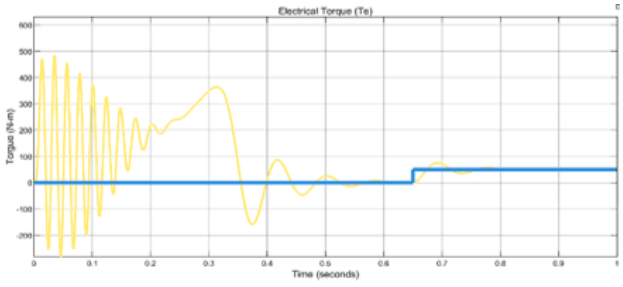

Figure 3: Graph of Electromagnetic torque against time

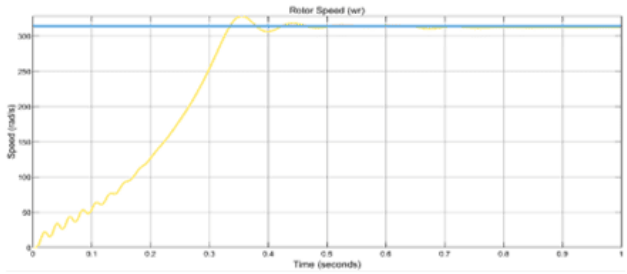

Figure 4: Graph of speed against time

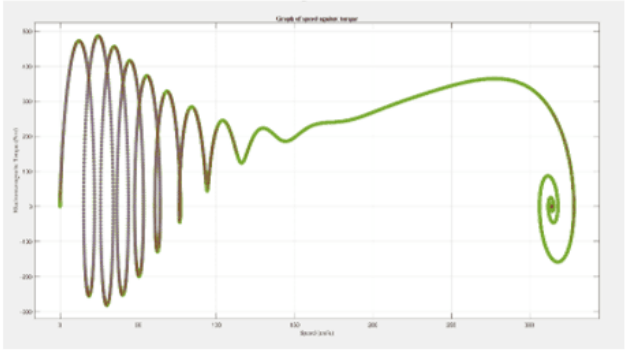

Figure 5: Graph of torque against rotor speed

5.3 Rotor Reference Frame

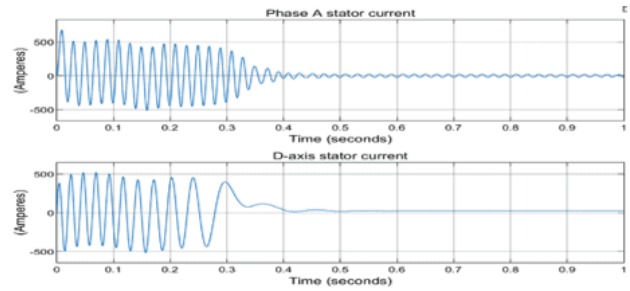

Figure 6: Phase A and d-axis stator current in rotor reference frame

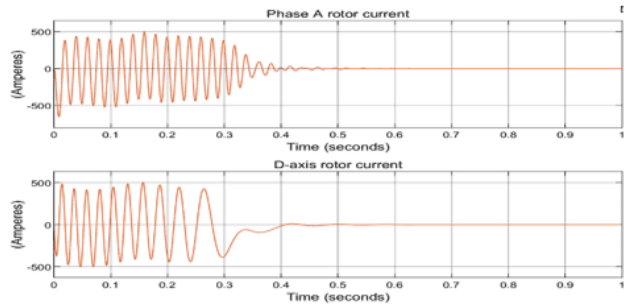

Figure 7: Phase A and d-axis rotor currents in the rotor reference frame

In the rotor reference frame, we = wr, and the direct axis of the reference moves at the same relative speed as the rotor phase A winding, coinciding with its axis. Therefore, the d-axis and phase A currents are identical, as shown in Fig. 6 and 7 above.

5.4 Stationary Reference Frame

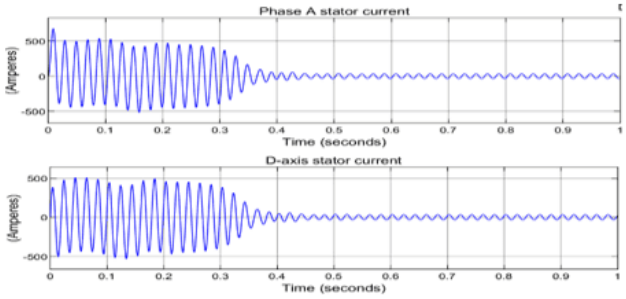

Figure 8: Phase A and d-axis stator currents in the stationary reference frame

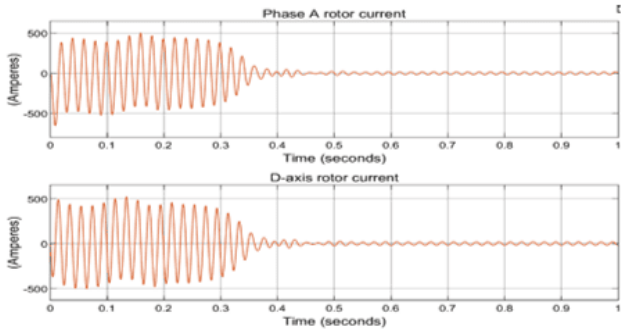

Figure 9: Phase A and d-axis rotor currents in the stationary reference frame

In this reference frame, w_e = zero, and the d-axis is aligned with the axis of the stator phase A winding, making them coincident. This means that the variables of the stator d-axis in this reference frame will behave the same way as the physical stator phase A variables of the motor. Figures 8 and 9 above illustrate the identical nature of the stator phase A current and the stator d-axis current.

5.5 Synchronous Reference Frame

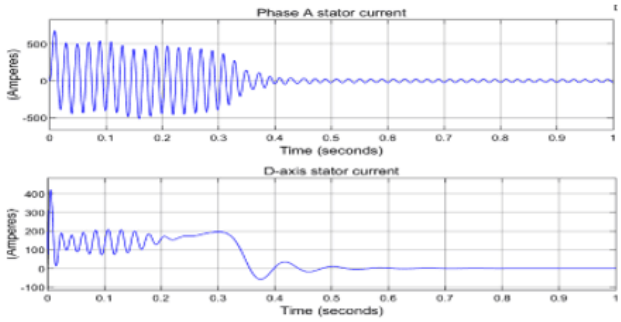

Figure 10: Phase A and d-axis stator currents in the synchronous reference frame

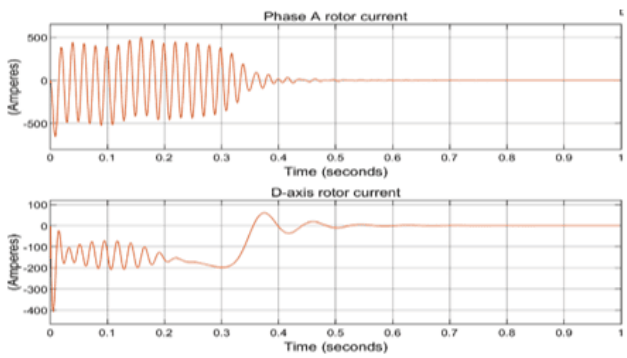

Figure 11: Phase A and d-axis rotor currents in the synchronous reference frame

When the reference frame rotates at the synchronous speed, both the stator and rotor are spinning at different speeds relative to it. The stator spins at the machine's rated frequency, while the rotor turns at its equivalent slip frequency. The d-q axis currents in this reference frame are entirely different for the stator and rotor Phase A currents, as shown in Figures 10 and 11 above.

5.6 Speed Under Balanced and Unbalanced Voltage Conditions

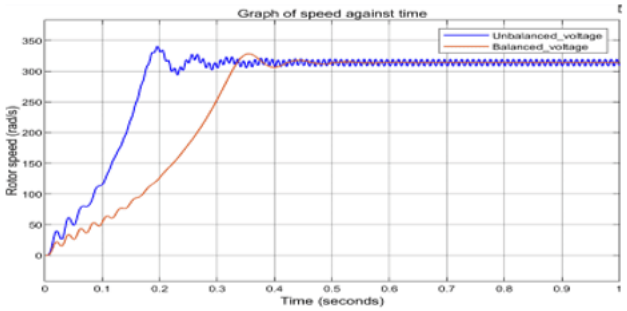

Figure 12: Graph of speed against time under balanced and unbalanced voltage conditions

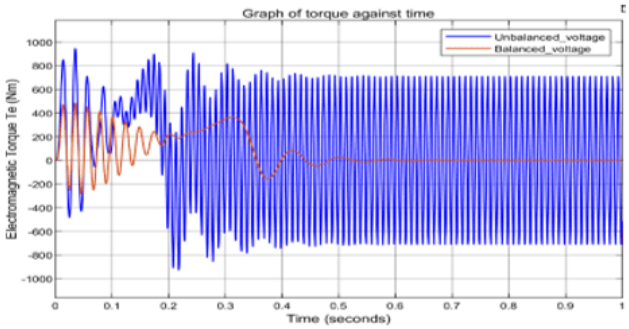

Figure 13: Graph of torque against time under balanced and unbalanced voltage conditions

The speed torque equations in the various reference frames demonstrate that, under unbalanced magnitude and phase of the supply voltage, a negative sequence component is created that produces a reverse magnetic field, resulting in increased losses, torque pulsations, and reduced efficiency. Overall, the impact of unbalanced voltage on the performance of the induction motor in the three frames of reference includes increased losses and heating, reduced efficiency, and torque pulsations, which can lead to increased noise and vibration, as well as a reduced motor lifespan.

The comparative analysis of the induction machine in the stationary, rotor, and synchronous reference frames, uncovers definite strengths, especially when dealing with balanced and unbalanced voltage conditions. With a balanced voltage condition, the torque versus speed curves look identical no matter the frame of reference, as the electromagnetic torque settles steadily around 49.73 Nm and the rotor speed reaches 1500 rpm in just 0.49 seconds under no-load conditions. Then, at 0.65 seconds, adding a load triggers small ripples in both metrics, as illustrated in Figures 3 – 5.

Conversely, under unbalanced stator voltages (e.g., 50 percent reduction in phase B magnitude), the rotor reference frame performs better by reducing torque pulsations to ±5 Nm, and speed dips to 2% below nominal value, compared to torque pulsation of ±15 Nm and speed dips of 5 – 7% in the stationary and synchronous reference frames, respectively as evidenced in Figures 12 – 13. This is owing to its alignment with rotor dynamics that inherently decouples unbalanced voltage condition-induced negative-sequence effects. Overall, these reference frame-specific behaviours highlights the d-q transformation's versatility.

6. Conclusion

This study analyses the dynamic performance of a three-phase induction motor using the d-q transformation in rotor, stationary, and synchronous reference frames, with a particular focus on torque-speed behaviour under both balanced and unbalanced voltage supplies. A flux-linkage-based modelling approach simplifies MATLAB/Simulink simulations. The study's results also indicate that the synchronous reference frame is best suited for balanced voltage conditions. In contrast, the rotor reference frame is suitable for unbalanced stator voltages, and the stationary reference frame is most ideal for unbalanced rotor voltages. Torque-speed characteristics are invariant across frames under balanced voltage conditions,

underscoring the efficacy of the d-q method. Future work may extend to fault-tolerant control strategies.

References

[1] Paul Krause, Oleg Wasynczuk, Scott Sudhoff, & Steven Pekarek. (2013). *Analysis of electric machinery and drive systems*. (3rd ed.). Hoboken, New Jersey: John Wiley & Sons, Inc.

[2] O. I. Okoro. (2004). Generalised program for the dynamic simulation of symmetrical induction machine. *Nigerian Journal of Tropical Engineering*, *5*, 16–24.

[3] Archibong E., Akisot E, Asuquo Eke, & Akpama E.J. (2021). *Performance, evaluation of three phase induction machine control using Simulink*. Available at: www.ijiset.com

[4] S. Gupta, & S. Wadhwani. (2007). *Dynamic modeling of induction motor using rotor rotating reference frame*. Available at: www.ijareeie.com

[5] R. J. Lee, P. Pillay, & R. G. Harley. (1984). D, Q reference frames for the simulation of induction motors. *Electric Power Systems Research, 8*, 15–26.

[6] Aleck W. Leedy. (2013). Simulink/MATLAB dynamic induction motor model for use as a teaching and research tool. *International Journal of Soft Computing and Engineering*, *3*(4), 102–108.

[7] E.J Akpama, & L.U. Anih. (2015). Modelling and simulation of multiphase induction machine. *International Journal of Engineering Innovation and Research, 4*(5), 732–737.

[8] B. Ozpineci, & L. M. Tolbert. (2003). Simulink implementation of induction machine model-A modular approach. *IEEE*, *2*(3), 728–734.

[9] B. Anand, & Dr. M.S. Aspalli. (2015). Dynamic d-q model of induction motor using simulink. *International Journal of Engineering Trends and Technology (IJETT)*, *24*(5), 252–257.

[10] Akpama E.J., E. E. Ekpenyong, & Oboho K. (2017). Performance evaluation of fuzzy logic control of induction motor. *World Journal of Engineering Research and Technology*, *3*(5), 1–10.

[11] Eko J Akpama, Iwara E. Omini, Emmanuel E. Effiong, & Raymond U. Ezenwosu. (2020). PID speed controlled model of induction motor using simulink. *International Journal of Engineering Research and Management*, *7*(10), 24–28.

[12] Lakhya Jyoti Phukon, & Neelanjana Baruah. (2015). A generalized matlab simulink model of a three phase induction motor. *Int J Innov Res Sci Eng Technol*, *4*(5), 2926–2934.

[13] C. J. O'Rourke, M. M. Qasim, M. R. Overlin, & J. L. Kirtley. (2019). A geometric interpretation of reference frames and transformations: Dq0, clarke, and park. *IEEE Transactions on Energy Conversion*, *34*(4), 2070–2083.

[14] O. I. Okoro. (2005). Dynamic modelling and simulation of squirrel-cage asynchronous machine with non-linear effects. *J ASTM Int*, *2*(6), 505–520.

[15] P. Daffin Onwe, E. James Akpama, O. I. Okoro, & E. N. Oku. (2015). *Dynamic behavior of asynchronous motor under balanced and unbalanced voltage source conditions*. Available at: www.wjert.org

[16] E. J. Akpama, O. I. Okoro, & E. Chikuni. (2010). Simulation of the performance of induction machine under unbalanced source voltage conditions. *The Pacific Journal of Science and Technology*, *11*(1), 9–15.

[17] J. S. Sokipriala, & Nwaorgu G O. (2021). Dynamic analysis of induction machine in various reference frame under balanced and unbalanced voltage conditions *International Journal of Advances in Engineering and Management (IJAEM)*, *3*(7), 3253–3258. DOI: 10.35629/5252-030732533258.

[18] A. Simion, L. Livadaru, & A. Munteanu. (2012). Mathematical model of the three-phase induction machine for the study of steady-state and transient duty under balanced and unbalanced states. In: *Induction Motors - Modelling and Control*. DOI: 10.5772/49983.